Neutral excited configuration of rare-gas atoms adsorbed on alkali metals

Doon Gibbs,* J. E. Cunningham, and C. P. Flynn
Department of Physics and Materials Research Laboratory, University of Illinois at Urbana-Champaign, Urbana, Illinois 61801
(Received 13 December 1983)

We report optical-excitation spectra of rare-gas atoms adsorbed on alkali-metal surfaces. The data were obtained with the use of differential reflectance methods with synchrotron radiation. Optical absorption appears to increase almost linearly from 0 at a well-defined excitation threshold energy that agrees quantitatively with the theoretical prediction for rare gases adsorbed on metals. The absorption continuum above threshold, for adsorbates distributed at dilution over the surface, is broken by the spin-orbit partner of the $P_{3/2}$ threshold process and by excitation to higher atomiclike configurations. Additional features which grow with coverage originate from adsorbate pairs. Both the threshold profile and pair peaks bear noticeable resemblance to the properties of rare-gas atoms alloyed into alkali metals, which have been investigated in earlier work. No theory is currently available to describe either the linear threshold profile or the pair peaks. The data establish unambiguously that the *neutral* excited rare-gas adsorbate configuration is created by the optical excitation, rather than the *ionic* configuration produced in photoemission work. These various properties are systematically described by a quantitative phenomenological model.

I. INTRODUCTION

The excitation spectra exhibited by foreign atoms adsorbed on metal surfaces shed light on two important areas of current research activity. First, one can determine what excited electronic configurations the adsorbed species adopt on the metal surface. Here the primary spectroscopic effort has focused on the way the substrate modifies levels of the free adsorbate, and on any new self-consistent excited configurations the adsorbate-metal interaction itself creates. Charge-transfer excitations are important examples of transitions to configurations which originate entirely from the adsorbate-substrate coupling. A second area of intense research effort concerns the response of conduction electrons to a shock which is localized at one atomic site. The change of local structure associated with core photoabsorption, for example, causes an abrupt alteration of local fields. One direct consequence of the change is that electron-hole pairs are excited in the conduction band. The spectrum of energies these additional processes require broadens the range of excitation energies over which transitions to a particular excited adsorbate configuration take place. Adsorbate excitation profiles therefore reflect both the spectrum of excited configurations accessible to the adsorbate and the way these excitations couple to the conduction-electron liquid of the substrate metal.

This paper is mainly confined to the subject of rare-gas atoms adsorbed on alkali-metal surfaces. In the paper that follows (hereafter referred to as paper II) rare-gas atoms on Al and Mg surfaces are discussed. From an experimental standpoint the alkali systems present severe disadvantages. Ultrahigh vacuum is required to maintain control of surface contaminants in the spectroscopy of adsorbed species on clean surfaces; for this purpose the high vapor pressures and extreme reactivity of alkali metals make them particularly unsuitable. Also, rare-gas atoms adsorb rather weakly on most metals, including the alkalis. To ensure that rare-gas atoms are adsorbed securely on alkali surfaces it is therefore necessary to undertake the added complication of substrates maintained at liquid-helium temperatures. The advantage that overwhelms these experimental difficulties is the theoretical simplicity of the rare-gas—alkali system. Rare-gas atoms and the alkali metals are paradigms for closed-shell molecules and simple metals, respectively. In addition, there is a special chemical simplicity about the excited configuration of an adsorbed rare-gas atom on an alkali metal, to which we turn in what follows. Thus the choice of rare gases adsorbed on alkalis is made in the hope that the properties of these, the simplest available adsorbate complexes, will help to clarify subtle and still unresolved problems that remain in the *theoretical* descriptions both of the excited configurations available to adsorbates and of the electron-liquid response to the excitation process.

Much information about rare gases on metal surfaces already exists. In a number of cases the heats of adsorption and the accompanying work-function changes have been determined.[1] Diffusion of rare-gas atoms on clean metal surfaces has been studied.[2]

Early investigations of photoemission from the adsorbed species revealed core-level shifts arising from the core-hole—substrate interaction.[3] More recently Chiang *et al.*[4] have measured the coverage dependence of rare-gas core-level shifts and the corresponding substrate work-function changes. Kaindl *et al.*[5] have explicitly identified the distance dependence of photoemission line shifts for an adsorbed layer. Certain structure on the photoemission peaks has been associated with crystal-field splitting of the $P_{3/2}$ core level by the image field of the

core hole.[6] Other work has identified broadening with dispersion of the core hole propagating from one adsorbate to the next in an ordered overlayer.[7] Further evidence that photoemission leaves behind an unneutralized core hole on these surfaces comes from the work of Gadzuk *et al.*[8] who observe and interpret vibrational broadening originating in the image field. Finally, a discussion of image formation by core-hole screening in the local-density approximation has been given by Lang.[9]

Rare-gas adsorbates have also been examined by differential reflectance,[10] Auger electron yield,[11] and electron-energy-loss spectroscopies.[12] These results differ among themselves and with the photoemission data. It seems clear that the various spectroscopies probe different phenomena, and this is reasonable since they correspond to different operators. However, the nature of these effects has remained still to be fully clarified. In earlier publications[13] we note that photoemission and optical-absorption processes may reach different final states, and that either an ionic or a neutral configuration may be the lowest excited level, depending on the particular metal and rare-gas atom.[10,13] Signs of the crossover were first reported from differential reflectance results for Xe, Kr, and Ar adsorbates on several substrates.[10] Since then the situation has become still less clear. Photoemission data and theory results have been interpreted to show that the ionic configuration still prevails where the optical results indicate the neutral configuration.[14] There is reason, however, to believe that neither the photoemission interpretation nor the theory is reliable (see the Appendix). Still further complexity arises from the fact that adsorbate transitions are coupled to the electrons in a conduction band. It is well known that photoemission spectra develop low-energy tails owing to the response of the metal, and that optical spectra broaden to high energy and become absorption edges.[15] The main theoretical descriptions have been given by Mahan and Nozieres and de Dominicis (MND)[15,16] for the optical process and by Doniach and Sunjic[15,17] for photoemission. A recent review is offered by Wilkins.[18] These theories appear to have had some success in describing optical line shapes for core levels in pure metals.[19] Unfortunately they appear unable to deal with impurity spectra, for reasons which are not yet understood. It is a particular problem that the theory fails badly for rare-gas atoms alloyed into the bulk of simple metals.[20] Therefore, while the spectral line shapes of rare-gas adsorbates are of special theoretical interest, one cannot expect that existing theories of the spectra will help in the interpretation of adsorbate properties.

Our purpose in the present paper is to present a unified view of the rare-gas adsorbate problem. There is no doubt that photoemission from adsorbed rare-gas atoms leaves the *ionic* rare-gas complex on many transition-metal surfaces, nor that this ionic configuration is the lowest excited configuration of the complex. In this paper we present new data and new calculations which establish unambiguously that on certain simple metal surfaces the *neutral* configuration is the lowest, and that it is created by direct optical excitations. We also discuss higher excited states in both regions and the relationship of these metastable levels to various experiments.

The plan of this paper is as follows. Section II describes a chemical understanding of adsorbate structure that can be obtained by the use of configurational models for the metal-adsorbate complex. In Sec. III the equipment employed in the research is described. Our experimental results are also presented and analyzed in accordance with the models described in Sec. II. Finally, in Sec. IV, we discuss and interpret the spectroscopic results. Data obtained for nonalkali substrates and by other spectroscopies are discussed and interpreted in paper II.[21]

II. ELECTRONIC STRUCTURE OF RARE-GAS ADSORBATES

It has been understood for many years that rare-gas atoms suffer only minor deformations when adsorbed in their ground states on metal surfaces. This is particularly true of alkali-metal substrates, for which case the metal-adsorbate complex has a negligible dipole moment.[22] Observed correlations between the dipole moment and the heat of adsorption lead one to estimate an equilibrium bonding energy $\lesssim 0.05$ eV between the Xe atom and a typical alkali metal.[1,22] Evidently the ground state of the complex consists of the two relatively undeformed metal and atom components.

It happens that the first excited state of rare-gas adsorbates also couples to the metal in a way which can easily be understood. Consider the example of Xe and Cs metal. The first excited state of Xe $5p^6$ is $5p^5 6s$. In this configuration the $(5p^5)^+$ core binds the $6s$ orbital in much the same way as does the $(5p^6)^+$ core of Cs $5p^6 6s$.[10,20] This analogy is the "$Z+1$ model," which identifies the valence structure of the core-excited atom with that of its neighbor to the right in the Periodic Table.[23] In the case of excited np^6 rare-gas atoms, the binding energy of the outer $(n+1)s$ level equals that of the neighboring $np^6(n+1)s$ alkali to within a very few percent. The chemistry of the rare-gas excited state interacting with metals can therefore be simulated quite accurately by analogy with the alkali metal. For rare-gas atoms alloyed into the bulk of alkali metals, for example, the excitation energies can be estimated to about ± 0.2 eV in about 10 eV.[20] The argument will be repeated here for the case in which rare-gas atoms are adsorbed on the surface. For these purposes, the properties in Table I prove useful.

Consider once more the case of Xe on Cs. As the p^6 ground state of the atom is brought up to the metal from infinity, the bonding is only some hundredths of 1 eV and may often be neglected. Since the excited state of Xe resembles a Cs atom, its equilibrium bonding to Cs metal as it reaches the surface is approximately the Cs cohesive energy. The optical-excitation threshold, as the difference between the total energies of the two configurations, is

$$\hbar\omega_0 = \hbar\omega_a - \epsilon \,, \tag{1}$$

in which $\hbar\omega_a$ is the excitation energy of the free adsorbate atom (here Xe) and ϵ is the difference of the excited-state and ground-state bonding to the metal. For the case of Xe on Cs we can neglect the ground-state bonding, and so, according to the $Z+1$ model, ϵ is the cohesive energy of the metal (here Cs). The relaxed, total energies of the

TABLE I. Properties (in eV) of rare-gas atoms and the predicted photoemission threshold $\hbar\omega_P$ and optical-absorption threshold $\hbar\omega_0$. The total energy E^* of the neutral excited configuration is also given, with respect to the energy zero of Fig. 1, in which the electron, the ion, and the metal are remote from one another. I and I^* are the ionization energies of the atomic np^6 ground state and the $np^5(n+1)s$ excited state, respectively, and $\hbar\omega_a$ is their difference, the atomic excitation energy (Ref. 24). Δ is the image energy deduced from the atomic radius and ϵ is the cohesion per atom of the alkali-metal neighboring the rare-gas atom in the Periodic Table (e.g., Cs for Xe, etc.).

	Ne	Ar	Kr	Xe
I	21.56	15.76	14.00	12.13
I^*	4.89	4.14	4.00	3.70
$\hbar\omega_a$	16.67	11.62	10.03	8.43
Δ	2.27	1.91	1.80	1.66
ϵ	1.11	0.93	0.85	0.80
E^*	−6.00	−5.07	−4.85	−4.50
$\hbar\omega_P$	19.29	13.85	12.20	10.47
$\hbar\omega_0$	15.56	10.69	9.18	7.63

ground and first excited configurations as functions of the metal-adsorbate spacing z are sketched in Fig. 1.

Note that Eq. (1) can be employed more generally to describe the excitation energy of *any* rare-gas atom on *any* alkali, provided that ϵ is taken as the cohesion of the pure alkali metal to whose atoms the excited rare-gas atom is equivalent.[23] This follows from the observation that the heats of intersolution among alkali metals are small, typically $\lesssim 0.1$ eV, so that each alkali atom coheres to any alkali environment much as in its own pure metal.[25] Of course, our treatment presupposes that optical transitions of the adsorbed species take place at values of z appropriate to bonding of the metal, whereas in practice they occur at the spacing for the adsorbed *ground* state. The error is a "Stokes shift" which displaces the mean absorption away from the threshold [Eq. (1)], but by a shift which is generally negligible for alkalis.[8,26] The results of Eq. (1), given in Table I, often predict the observed threshold energies to within $\sim \pm 0.1$ eV (see Sec. III).

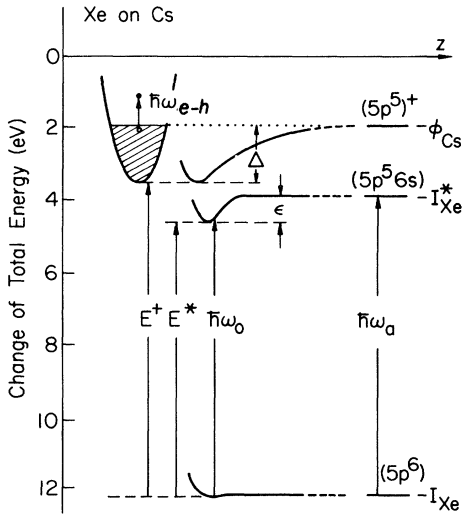

FIG. 1. Energetics of three Xe configurations interacting with the surface of Cs: the $5p^6$ ground configuration, the $5p^56s$ first excited configuration Xe*, energy E^*, and the $(5p^5)^+$ charge transfer configuration, each shown schematically as a function of Xe distance z from the Cs surface. The figure shows changes of *total* energy of the configurations, including conduction-band excitations. Configurational energies are with respect to a zero in which the $(p^5)^+$ ion, the electron, and the metal are far apart. Conduction-band excitations $\hbar\omega_{e\text{-}h}$ add to the total energy, and the band is correctly shown to represent energy changes when an electron is removed from the metal, as in photoemission. By accident, for Xe on Cs, $\Delta \simeq E_F$, but this is not generally the case.

In the preceding discussion we have allowed the conduction electrons of the metal to remain in their lowest-energy configuration for any z. However, a complete description of any particular excited state of the metal-adsorbate complex can only be obtained when the excited configuration of the adsorbate and the excitation state of the conduction electrons are *both* specified. On the left-hand side of Fig. 1 is included a conduction band with its quasiparticle levels, so that the energy-level difference gives the total energy required for the electron-hole excitation; an example is indicated by the arrow $\hbar\omega_{e\text{-}h}$. The conduction band is positioned with E_F below the vacuum level by the work function ϕ, so that the total energy required to remove a conduction electron to infinity is correctly represented. The advantage of Fig. 1 is that simple excited configurations of the metal-adsorbate complex can easily be specified.

One necessary complication Fig. 1 introduces is that the excitation energy is the sum of the adsorbate configuration change (e.g., arrow $\hbar\omega_0$ in Fig. 1) and the excitation energy of the conduction electrons (e.g., arrow $\hbar\omega_{e\text{-}h}$ in Fig. 1). The basic configurations can be produced by creating the complex adiabatically from the metal with a given state of the atom. However, the shock of an optical event in the coupled system may create additional excitations of the conduction states, as modeled here by $\hbar\omega_{e\text{-}h}$.[15]

It is interesting to inquire whether or not higher excited states of the atom can remain visible in the adsorbate spectrum. For the cases of direct interest here the answer is that excited configurations derived from other *core holes* may well be observable, but the *higher orbital excitations* with the same core hole become parts of the metal absorption continuum. Our example of Xe on Cs once more makes this clear. When Xe* $5p^56s$ is adsorbed on Cs its $6s$ state, being Cs-like, is mixed fully into the Cs $6s$-derived conduction band. Just as for the Cs host atoms, higher Xe* excited orbitals such as $7s$, $8s$, etc., become the excited Bloch states of the metal. Thus Xe on Cs has only one excited neutral configuration, together with the electron-hole excitation continuum of the conduction-electron liquid. In these simple systems it is perhaps always the case that, when the lowest excited orbital mixes fully into the conduction band, the higher atomic orbitals merge into the virtual Bloch states.

The preceding employs single-particle concepts such as degenerate mixing and orbital energies in a discussion previously restricted to total energies and many-particle con-

figurations (a possible ambiguity for conduction-band excitations is permissible because Koopman's theorem is valid for delocalized band states). An unconsidered use of these ideas can cause endless confusion. To understand single-particle mixing it is helpful to use Wigner-Seitz ideas in which exchange and correlation energies are approximately accommodated by keeping conduction electrons in separate cells,[27] and with rigid ion cores. The band bottom energy (frequency) is thus lowered from that of the atom by the cell boundary modification; the added kinetic energy of the conduction electrons brings E_F back near the atomic level. This makes the net cohesion $\epsilon \simeq \frac{2}{5} E_F$ (see Fig. 2), which agrees well with experiment for the alkali metals.[27] These useful concepts make it possible to assess whether or not two electrons with similar energies (frequencies) in neighboring systems will *exchange.* They give conduction-electron energies for the Cs band in the range -3.9 to -5.5 eV. In contrast, Fig. 1 displays the Cs band in the range -1.9 to -3.5 eV for electrons which have been *extracted from the metal.* The distinction between the two cases is that surface effects cancel from the exchange of two particles having similar frequencies, but do modify the work required to remove one particle. Some further discussion of related points will be found in Appendix I.

Figure 2 compares estimated conduction-band ranges for the alkali metals with the ionization energies I^* of rare-gas excited states when lowered by their alkalilike cohesion. As expected, the alkalilike adsorbate levels lie in the same energy range as the band states of alkali metals, and the two therefore mix together.

A different excited configuration of the metal-adsorbate complex warrants further comment. This is the ionic state Xe^+ obtained when the $6s$ orbital of Xe* is removed from the atom and placed in the metal. The work required when z is large is *exactly* $I^*-\phi$, with I^* the $6s$ ionization energy of Xe* and ϕ the metal work function. In Fig. 1 the zero of energy corresponds to the state in

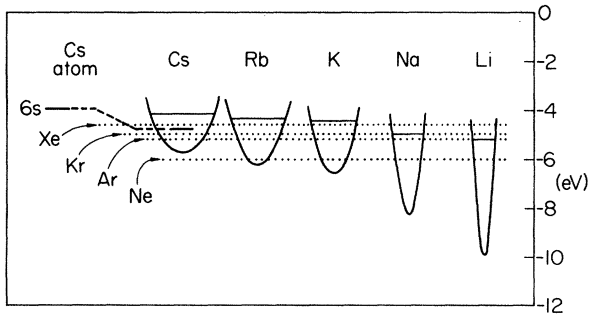

FIG. 2. Conduction energies of electrons in alkali metals and in adsorbed rare gases in their neutral excited configurations, showing how the two fall in the same energy ranges. The alkali band states are lowered from the ionization energies of free atoms by the alkali-metal cohesive energy, and spread by E_F about this mean energy. The adsorbate states are lowered by the alkalilike cohesion from the ionization energies of the excited rare-gas atoms. The figure indicates that the excited orbital of the neutral excited configurations of rare-gas atoms generally mix into the conduction bands of alkali-metal substrates.

which the metal, the electron, and the Xe^+ ion are all remote from each other, so that the Xe* configuration tends to $-I^*$ and Xe^+ to $-\phi$ as $z \to \infty$. The point of principal interest emerges as z is reduced and the total energy of the Xe^+ configuration is changed by the interaction Δ between the ion and the metal. A fairly good approximation is to model this interaction using only the "image" energy $e^2/4z$. We shall write

$$\Delta \simeq e^2/4r \tag{2}$$

for the energy at the equilibrium spacing when the ion is spaced from the metal by its radius r. This amounts to 1.5–2 eV for Xe, which has a radius $r \simeq 2$ Å.

We wish to obtain an expression for the work needed to remove an electron from the adsorbate on the metal. This will give the photoemission threshold, $\hbar\omega_P$, namely, the lowest photon energy which can excite an electron into the vacuum from the adsorbate core. In the free atom, the work required is, by definition, the ionization energy I. Energy Δ is available as the free ion approaches the metal; as this energy is released, less photon energy is required to eject the electron. At the equilibrium position

$$\hbar\omega_P = I - \Delta \, . \tag{3}$$

As in Eq. (1), this simple expression neglects ground-state bonding, but is very useful and surprisingly accurate. No data are currently available for photoemission from rare-gas atoms on alkali metals, where the ground-state bonding is weakest and Eq. (3) is best justified. Even for the $3p$ shell of Ar on Al, discussed in Appendix I, Table I gives $\hbar\omega_P = 13.85$ eV while the measured value is 14.1 eV. Chiang *et al.*[4] discuss deep levels and the apparent effect on Δ.

It is necessary, also, to calculate the difference of total energy between the neutral configuration and the ionic configuration. Starting with the ion, the metal, and the electron all remote from each other, the neutral configuration is obtained by placing the electron on the atom, thereby releasing I^*, and bringing the excited atom up to the metal, releasing ϵ, so that the total energy of the neutral system is

$$E^* = -I^* - \epsilon \, . \tag{4}$$

For the ionic system, the electron is placed in the metal releasing ϕ, and the ion brought up to the metal, releasing Δ; its energy is therefore

$$E^+ = -\phi - \Delta \, . \tag{5}$$

In this way one finds the splitting

$$E^+ - E^* = I^* - \phi + \epsilon - \Delta \tag{6}$$

between the total energies of the two configurations. For Xe on Cs, $\epsilon = 0.80$, $I^* = 3.70$, $\phi = 1.9$, and $\Delta \simeq 1.66$ eV (see Tables I and II), so $E^+ - E^* = -0.94$ eV. Evidently, the Xe* complex is stable with respect to Xe^+ for Xe on Cs. This situation is reversed for certain other substrates.

As with the ground-state and first excited configuration, the charge transfer configuration possesses a spectrum of additional conduction-electron excitations. The conduction states are deformed differently near each con-

TABLE II. Relative stability (in eV) of the neutral $np^5(n+1)s$ excited configuration, energy E^* (eV), of adsorbed rare gases and the ionic $(np^5)^-$ charge transferred configuration, energy E^+. The values of ΔE are obtained from the properties in Table I and from the values (Ref. 29) of ϕ in column 1. It is expected that the results for ΔE are accurate to a few tenths of 1 eV.

	$\Delta E = E^+ - E^*$			
Substrate (ϕ eV)	Ne	Ar	Kr	Xe
Cs (1.9)	1.83	1.26	1.12	0.94
Rb (2.2)	1.53	0.96	0.82	0.64
K (2.3)	1.43	0.86	0.72	0.54
Na (2.4)	1.33	0.76	0.62	0.44
Li (2.9)	0.83	0.26	0.12	−0.06
Mg (3.7)	0.03	−0.54	−0.68	−0.86
Al (4.2)	−0.47	−1.04	−1.18	−1.36
W (4.5)	−0.77	−1.34	−1.48	−1.66
Au (5.1)	−1.37	−1.94	−2.08	−2.26

figuration of the adsorbate; this alters matrix elements for excitations but leaves the density of available excited band levels almost unchanged. In this same connection it is worth mentioning that the configurational labels Xe*, Xe^+, etc., specify precise characteristics only for z large. As z is reduced and interactions occur, the configurations of the complex evolve as exact diagonalizations of the metal-adsorbate Hamiltonian and, in general, can no longer be assigned integral charge characteristics, etc.[13]

It is useful to quantify the range through which $E^+ - E^*$ varies among different examples. Table II lists some cases. It is smallest for Xe on Au with $E^+ - E^* = -2.26$ eV, and largest with a value of 1.83 eV for Ne on Cs. These, together with cases which are relevant to the experiments reported in this paper, are detailed in Table II. It is our expectation that the predictions for the excitation energy to the neutral configuration are accurate to ~0.1 eV (since it is easier than for bulk alloys, where the typical uncertainty is ±0.2 eV) and that the predictions for the ionic configuration have significantly larger uncertainties. These arise in part from the systematic possible error in selecting appropriate values of ionic radii.

We remark that although the alkali metals used in this work are quench condensed, and therefore imperfect, this should not affect the energetics discussed here to any considerable extent. The electrical resistances of the quench-condensed alkalis correspond to defect structures with ~1–2% vacancy content.[20] This should entail a cohesion change also ~1%, which therefore shifts the excitation energies by only ~0.01 eV. In summary, therefore, these arguments probably predict the neutral excitation threshold to ~0.1 eV. The splitting between the ionic and neutral configuration is probably uncertain to a few tenths of 1 eV in a range of $E^+ - E^*$ which varies through ~4 eV.

Setting the electronic structure problem aside we now turn to a brief discussion of the optical-excitation characteristics. The simple example of Xe on Cs again provides a clear illustration of various possible phenomena. First, the $Xe(5p^5)^+$ core is very similar to the $(5p^6)^+$ core of the Cs ground state. Therefore, the Cs $6s$ conduction band must extend out from the Cs surface to overlap the Xe $5p$ hole of the excited adsorbate, just as it would happen for a Cs adatom. It follows that the Xe $5p \rightarrow 6s$ resonance transition remains strongly allowed in the coupled adsorbate-metal system. As mentioned earlier, the higher excited orbitals of the atom must be replaced in the complex by virtual Bloch orbitals. Accordingly, the electronic spectrum is expected to start with a well-defined threshold (the energy of the neutral excited configuration) and to extend as a continuum to higher energies through the mechanism of conduction-band excitations.

One might expect to describe such strongly allowed transitions in a metal using MND theory[15] (see Sec. I). For the bulk metal it turns out that the $np^6 \rightarrow np^5(n+1)s$ resonances of rare gases in alkali metals are predicted to have sharply peaked absorption at excitation threshold, followed at higher energy by an absorption continuum.[20] Instead, the observed spectra show suppressed thresholds (which nevertheless occur at the expected energy), followed at higher energy by a linearly increasing intensity of absorption.[10] There exists at present no explanation for the serious disagreement between theory and experiment. While it is therefore pointless to dwell on theoretical assessments of the analogous adsorbate problem, the failure of the theory for the bulk impurity does add extra interest to the spectra that rare-gas atoms exhibit when coupled to the surfaces of the metal. These are reported in Sec. III.

Before discussing the experiments we note that the spectral profile of the photoemission process is of considerable interest also. The response of a metal to a local shock can involve plasmon excitations in addition to electron-hole pair creation. This is neglected in standard "many-body" treatments of the response[15–18] although the plasmon effects have been identified and discussed[28] in connection with certain bulk photoemission experiments. The central difficulty for a comprehensive theory is that metallic screening involves momentum transfers $\sim 2k_F$ at which plasmons and single electron-hole pairs no longer provide independent long-lived basis states.

It is nevertheless of considerable fundamental interest to understand the structure of the screening response for each particular experiment. In the case of photoemission from adsorbates we point out elsewhere[13] that the optical matrix elements at threshold naturally connect to the *ionic*

excited configuration of the adsorbate. Therefore, the response necessarily involves relaxation in the field of the freshly created ion. While a precise theory remains remote, the phenomenology of this response is straightforward. This behavior is discussed further in Sec. IV B. It appears possible to conclude from the experiments that the image response to the creation of rare-gas ions in photoemission mainly involves surface-plasmon creation, rather than quasiparticle pairs. This is in accordance with phenomenological models which have previously been employed to discuss adsorbate properties.[29]

III. TECHNIQUES AND RESULTS

A. Experimenal techniques

The data presented below were obtained by means of differential reflectance spectroscopy in the energy range 5—20 eV using synchrotron radiation. The main experimental techniques employed here have been described elsewhere[10] and are summarized briefly in what follows.

Differential reflectance measurements compare the light intensity reflected from a clean film with that reflected from an identical film supporting a known adsorbate coverage. In practice, adsorbates were deposited through a cold-shuttered nozzle onto one-half of an alkali film freshly evaporated from an outgassed stainless-steel boat. This film was prepared on top of a Mg reflecting layer which was itself freshly deposited on a sapphire substrate anchored near liquid-He temperature in an ultrahigh vacuum (see Fig. 3). Typical alkali-film thicknesses ranged from 50 to 200 Å; typical base pressures during evaporation were in the high 10^{-9} Torr range. Except during brief sample preparation periods, the alkali surfaces were enclosed successively by liquid-He and liquid-nitrogen temperature cans penetrated only by small light ports. The pressure at the sample surface was estimated to be well below 10^{-10} Torr during optical scans. No signs of sample contamination could be detected in the data over protracted measurement periods.

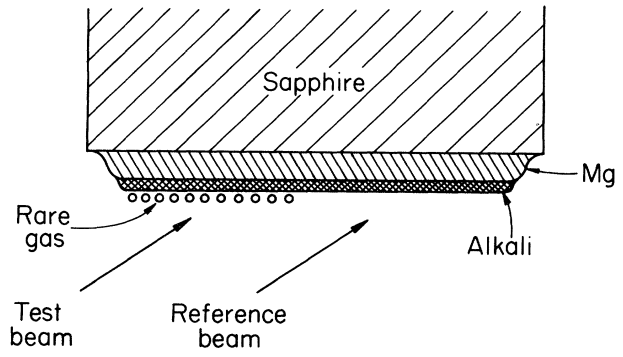

FIG. 3. Schematic diagram showing the sapphire substrate and successive Mg and alkali-metal films, freshly prepared *in situ*, together with the rare-gas adsorbate coverage that intersects the optical test channel but not the reference channel. The entire assembly is maintained near liquid-He temperature in a cryoshield held at liquid-He temperature.

Light from the University of Wisconsin Tantalus storage ring passed through a monochromator and was chopped into two parallel beams, one incident, on each of the two substrate halves. The reflected beams were detected using a single photomultiplier tube and the resulting signal measured by means of a lock-in amplifier. The normalized difference between the two channels was calculated and stored by means of a Texas Instruments 960 computer. Both source and photomultiplier drift are eliminated from the signal by these methods.

A useful advantage of this arrangement for the materials studied here is that the differential reflectance is proportional to the adsorbate optical absorption with very good accuracy. The alkalis are nearly transparent in the energy range 7—15 eV. Calculations of the differential reflectance using the classical formula of McIntyre and Aspnes[30] bear out this proportionality to better than 5%.[10] The most convincing confirmation of these ideas, however, is the fact that the measured spectra of alkali and rare-gas adsorbates at high coverage reproduce in a satisfactory way the spectra of the bulk solids. In what follows the spectra are therefore discussed without further comment as absorption data for the metal-adsorbate complexes.

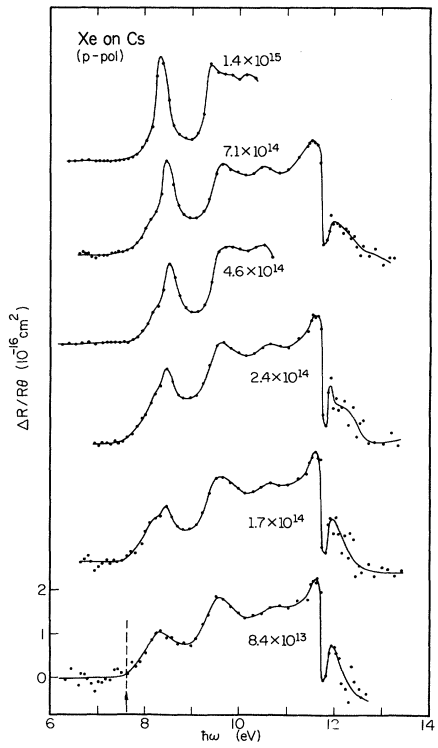

FIG. 4. Differential reflectance spectra of Xe on Cs at various coverages (in cm^{-2}). The spectra measure absolute absorption introduced by the Xe surface species, normalized to unit adsorbate coverage of 10^{15} cm^{-2}. Main features are the Xe $O_3, O_2, (5p^6 \rightarrow 5p^5 6s P_{3/2}, P_{1/2})$ processes and the O_3 edge of surface Cs atoms. The latter appear *negative* as the edge for surface Cs atoms coupled to the adsorbate is shifted away in energy. A vertical dashed line indicates the theoretical threshold energy (see text).

B. Results

Figure 4 shows the absorption by Xe adsorbed on Cs as a function of incident photon energy and of adsorbate coverage given in atoms cm^{-2}. The data have been scaled to display the absorption per atom. For this purpose the signal was divided by the coverage in units of 10^{15} cm^{-2}.

In the profile for $\Theta = 8.4\times10^{13}$ cm^{-2}, the peaks centered at 8.35 and 9.6 eV are associated with the spin-orbit split $5p^6 \rightarrow 5p^5 6s$ ($J=1$) excitations which occur at 8.43 and 9.57 eV in the free Xe atom.[31] The $P_{3/2}$ structure has an asymmetric form with a significant portion of the rising shoulder relatively linear at higher coverage. The threshold energy of 7.6±0.1 eV agrees perfectly with that predicted in Table I for the neutral excited configuration. Above 9.6 eV are higher excitations, continuing to an abrupt edge at 11.8 eV, which is associated with the Cs O_{23} core threshold for $5p^6 6s \rightarrow 5p^5 6s^2$ excitations. The line shape of the $P_{1/2}$ excitation at 9.0 eV and of the $d \rightarrow p$ excitations, centered near 10.5 eV, are obscured by absorption features peaked at lower energy.

At coverages greater than $\Theta \sim 1.4\times10^{14}$ cm^{-2} a sharp, excitonlike absorption peak emerges near 8.45 eV, above the linear profile. As the coverage is increased the peak accumulates oscillator strength approximately as Θ^2 so that it depends approximately linearly on Θ in the normalized spectra. Figure 5 shows the peak height as a function of coverage. At the same time, the peak center red shifts slightly with increased coverage to 8.35 eV, which is the energy of the $P_{3/2}$ exciton line of solid Xe.

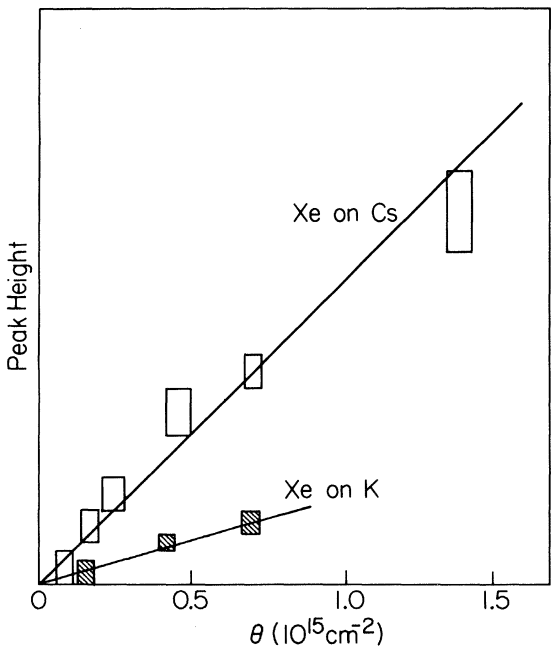

FIG. 5. Amplitude of the Xe $P_{3/2}$ pair peak as a function of coverage for Cs and K. The peak height is shown normalized, scaled by the coverage Θ (in units of 10^{15} cm^{-2}) as in Figs. 4 and 6. The linear dependence on coverage that remains indicates that the peaks vary as Θ^2 and thus arise from Xe pairs containing two Xe adsorbates at neighboring sites on the metal surfaces.

The integrated oscillator strength of the normalized profile remains satisfactorily constant over the entire range of coverages.

The data show that the asymmetric linear profile at low coverage is characteristic of the isolated neutral adsorbate. The peak excitonlike structure must originate from interacting Xe *pairs*. Xe pair excitations have previously been observed in the spectra of rare-gas–alkali bulk alloys[20] and for Xe on the surfaces of Mg, Al, and Au.[10] Note that the spectrum of the isolated adsorbate persists, though weakened, underneath the pair peaks as an independent excitation channel even at coverages approaching 1×10^{15} cm^{-2}.

The same linear, asymmetric line shape observed on Cs recurs when Xe is isolated on the surface of K, as shown in Fig. 6. The threshold at 7.6±0.2 eV for $\Theta = 1.5\times10^{14}$ cm^{-2}, and the positions of the $P_{3/2}, P_{1/2}$ line structures at 8.45 and at 9.55 eV, are nearly identical to those for $\Theta = 1.7\times10^{14}$ cm^{-2} Xe on Cs. These pair peaks appear in spectra for $\Theta \gtrsim 1.4\times10^{14}$ cm^{-2}; the $d \rightarrow p$ derived peak centered near 10.5 eV for Cs is also repeated in the K data. Only the abrupt change at 11.8 eV, associated with the Cs $5p$ core edge, is absent on K. The strong absorption above 12 eV may be associated with the Xe ionization limit which occurs at 12.1 eV in the atom.

Spectra for Kr on K are shown in Fig. 7. The atomic $4p^6 \rightarrow 4p^5 5s$ ($J=1$) excitations at 10.03 and 10.64 eV appear almost unshifted from the pair peaks centered at 10.05 and 10.7 eV in the data. Excitonic processes seem to occur at lower coverages for Kr than for Xe, with solidlike Kr peaks already apparent at 8.1×10^{13} cm^{-2}. The dashed line indicates the estimated profile of the isolated adsorbate. Its shape resembles that of Xe on K and Cs to a remarkable degree, including the threshold red shift of about 1 eV to 9.1±0.1 eV. The prediction in Table I is 9.2 eV. In the spectra of Kr on K, the $d \rightarrow p$-like excitations occur as a broad, sloping shoulder which begins near 12 eV.

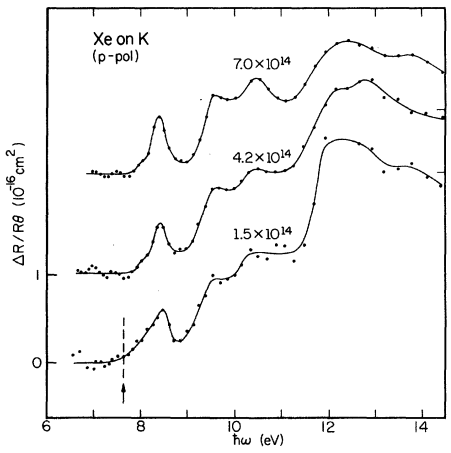

FIG. 6. Differential reflectance spectra for Xe on K at various coverages (in cm^{-2}) showing the Xe $O_3, O_2 (5p^6 \rightarrow 5p^5 6s P_{3/2}, P_{1/2})$ processes. The spectra measure the absolute absorption introduced by the adsorbate species normalized to unit adsorbate coverage of 10^{15} cm^{-2}. A vertical dashed line indicates the theoretical threshold energy (see text).

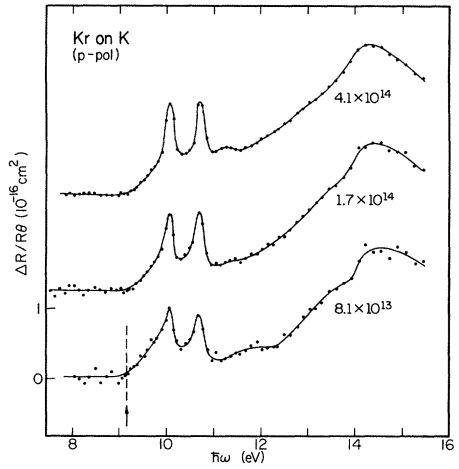

FIG. 7. Differential reflectance spectra of Kr on K at various coverages (in cm^{-2}), showing the Kr $N_3,N_2(4p^6 \rightarrow 4p^5 5sP_{3/2},P_{1/2})$ processes. The spectra measure the absolute absorption introduced by the Kr surface species, normalized to unit adsorbate coverage of 10^{15} cm^{-2}. A vertical dashed line indicates the theoretical threshold energy (see text).

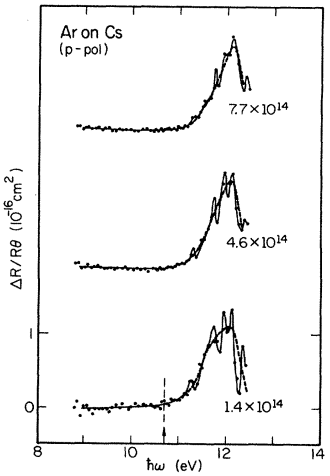

FIG. 9. Differential reflectance spectra for Ar on Cs at various coverages (in cm^{-2}) showing the Ar $M_{3,2}(3p^6 \rightarrow 3p^5 4sP_{3/2,1/2})$ process. The spectra measure the absolute absorption introduced by the Ar surface species, normalized to unit adsorbate coverage of 10^{15} cm^{-2}. A vertical dashed line indicates the theoretical threshold energy (see text).

Spectra for Ar on K and Cs are shown in Figs. 8 and 9. In the K results of Fig. 8, the Ar spectra appear to have an initially linear profile starting from a threshold near 10.9 eV, although the data for the lowest coverage are, unfortunately, too noisy to fix the behavior at dilution unambiguously. The observed threshold agrees quite well with the value 10.7 eV predicted in Table I for the neutral configuration. The broad trend of oscillator strength (dashed lines) indicated by the data of Fig. 9 for Ar on Cs is quite similar to that in Fig. 8. The Cs data were taken about a year later than the K runs and with improved resolution and signal-to-noise ratio. It is noticeable, however, that the actual data points trace a sharply structured curve (solid line) rather than the average trend of the dashed line. This structure may possibly originate spuriously in multiple reflection interferences of some type. We are inclined to believe, to the contrary, that the effect is adsorbate induced since it is not present in the absence of the adsorbate and its magnitude increases with coverage.

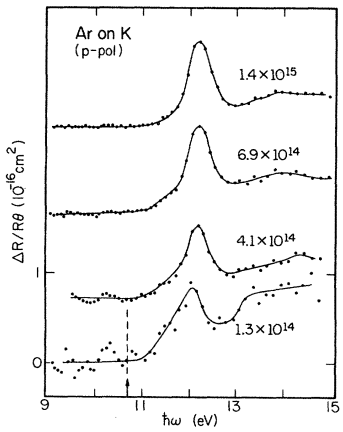

FIG. 8. Differential reflectance spectra for Ar on K at various coverages (in cm^{-2}) showing the Ar $M_{3,2}(3p^6 \rightarrow 3p^5 4sP_{3/2,1/2})$ process. The spectra measure the absolute absorption introduced by the Ar surface species, normalized to unit adsorbate coverage of 10^{15} cm^{-2}. A vertical dashed line indicates the theoretical threshold energy (see text).

The sharp negative spike in Fig. 9, which begins near 12 eV and is largest near 12.2 eV, is very probably the O_{23} edge of Cs atoms coupled to the Ar adsorbates, precisely as in Fig. 3 for Xe on Cs. It is certainly blue shifted from the expected location near 11.8 eV. Other peaks also occur in the spectra. One possibility is that the adsorbate and surface-metal atom excitations interact and mix to produce this structure. Certainly, the atomic Ar excitation at 11.62 and 11.8 eV fall very close to the O_{23} edge of Cs metal, near 11.8 eV. An alternative explanation which appears equally plausible is that the rapid change of dielectric function casued by the Cs O_{23} edge modifies the Ar-induced changes of reflectivity and produces the extra oscillations spuriously.

IV. DISCUSSION

The Hartree-Fock ideas discussed in Sec. II suggest that two regimes of behavior exist for rare-gas atoms adsorbed on metal surfaces.[10,13] In one, the lowest excited configuration is ionic with the excited electron transferred to the substrate; in the other, the lowest excited configuration is neutral. Doubt has been expressed about the second regime in the recent literature.[4,14] For this reason, the principal purpose of the present paper is to establish in a definitive way, first, whether or not a neutral configuration exists and, second, if it does exist, whether it constitutes the lowest excited configuration over the predicted range of parameters. In what follows we therefore examine the experimental evidence (Sec. III) in the light of the theoretical ideas (Sec. II) in order to assess the results. Following

this main issue, the discussion turns briefly to a number of secondary points. These include the possible existence of alternative excited configurations, the results of photoemission spectroscopy, and the question of optical line shapes.

A. Neutral excited configuration

The results of Sec. II indicate that all the systems examined in the experimental work reported here belong to the regime in which the first excited state is neutral. This is the case when $I^* + E_c > \phi + \Delta$. The weakest bound orbital is Xe*6s, for which $I^* + \epsilon = 4.6$ eV. With $\Delta \simeq 1.6$ eV the Xe* configuration is evidently stable for $\phi \lesssim 3.0$ eV. This holds for all alkali substrates. Li, with $\phi = 2.9 \pm 0.1$ eV, lies close to the instability.

Note, nevertheless, that a surprisingly wide range of one-electron structures occurs in the predicted regime of neutral stability. Figure 2 suggests that the 3s level, near -6.06 eV, of Ne* adsorbed on Cs, lies below the Cs band bottom (-5.5 eV) as a fully bound state. Xe* on Li is the opposite extreme for which the 6s orbital at approximately -4.6 eV lies well above the Fermi level of Li, near -5.3 eV. Presumably the 6s energy and occupancy are both fractionally lowered as the orbital spreads partly into the metal.

In contrast to these extremes, the cases of Xe, Kr, and Ar on metallic K, and Xe and Ar on Cs, reported in Sec. III, fall in the range where the neutral state is predicted to be stable and the excited orbital is degenerate with the conduction-band orbitals. The alloy analogy is therefore fully justified, and it is satisfactory that the excitation energies reported in Sec. III agree so well with the theoretical predictions. For the five cases examined here the energy at which the onset of $P_{3/2}$ absorption occurs agrees with that predicted with a maximum error of 0.2 eV. The position of the $P_{1/2}$ spin-orbit split replica is equally consistent with the model predictions. Also, the absolute oscillator strengths reproduce systematically.

The accurate predictability of the observed optical thresholds strongly affirms that the neutral excited configuration does occur in these systems. This result is further strengthened by the fact that the predicted ionic configuration lies at higher energy up to 1.3 eV. Moreover, the spectra provide detailed evidence that the samples are correctly prepared. Thus the coupling of the excitation to the conduction electrons is apparent both in the continuum absorption exhibited by each adsorbate above its excitation threshold and in the visibly perturbed spectra of the surface host metal atoms which are bound to the adsorbates (Figs. 4 and 9). The coupling is also to be inferred from the similar linearlike profiles evident immediately above threshold in the rare-gas spectra. Evidence that the adsorbates are randomly arranged and not grouped in two- or three-dimensional clusters comes from the linear variation with coverage of the "pair peak" intensities. The combined weight of the evidence therefore leads us to state that *the experimental and theoretical facts fully establish the existence of the neutral excited configuration* in these systems.

It warrants special emphasis that the configurations behave in such a simple way. Neither the optical threshold nor the photoemission threshold depend very sensitively on the particular substrate metal [see Eqs. (1) and (3)]. As a consequence, the crossover of total energies for the Xe* and Xe^+ complexes, described in Sec. II, tracks entirely with the change of ϕ from one substrate to the next. As ϕ is normally not in doubt, the predicted behavior of the total-energy difference appears securely founded. The recent literature contains commentaries in which one electron and total energies are confused together in a discussion of rare-gas adsorbate excitations.[14] The errors involved are explained in the Appendix.

B. Photoemission and the ionic excited configuration

It is not surprising that the data of Sec. III show no signs of transitions to the ionic excited configurations 0.5 to 1.3 eV above the neutral thresholds. The fact that the electron is transferred to the substrate means that little or no overlap of the valence electron with the rare-gas core persists in the ionic state. Therefore, as we point out elsewhere,[13] the optical matrix element is very weak. The lowest strong optical matrix elements to the charge transferred state connect to electron orbitals having positive energy with respect to the continuums, which *do* overlap the atomic core. These are photoemission processes which eject a propagating electron into the metal or the vacuum.[13]

One may inquire whether the ionic configuration still remains well defined when the neutral configuration is lowest. If so, its energy should be revealed by photoemission measurements on alkali—rare-gas complexes. The converse case, namely, possible persistence of the atomic configuration when the total energy of the ionic state is lowest, can already be established, for example, by the case of Ar on Al mentioned in the Appendix and discussed further in paper II.[21] A model of metastable state formation is discussed by Shinjo *et al.*[29]

It appears possible that the ionic configuration may persist above the neutral lowest excitation provided that no large single-particle matrix elements couple the two configurations. To see how this can occur, suppose that the complex is in the ionic state, so that the empty valence orbital is raised in energy by the image potential 2Δ. An electron can tunnel into the empty level from the conduction band only if the level still lies below E_F. In the absence of the image field it must thus lie 2Δ or more *below* E_F. Figure 2 reveals not a single case in which the orbital is bound so deeply. Therefore, it seems likely that the ionic configuration, once created, can persist for an extended lifetime. These possibilities may be explored by future photoemission experiments on alkali—rare-gas complexes.

The structure of the photoelectron spectrum is also of considerable interest. In an ideal experiment, the core electron is ejected so rapidly that the remaining system can be regarded as frozen. This creates an unscreened charge near the metal. The subsequent response of the metal lowers the energy by the image energy Δ, as described in Sec. II. This energy, however, is stored in the form of excitations of the metal. Since the photoemission peaks do seem to shift by about Δ (Sec. II), it appears that

this energy-absorbing response is not, in fact, fully reflected in the shift of the observed photoemission peak. Quasiparticle pair creation processes[15–18] and phonon sidebands[8,25] are essentially continuums which could not avoid detection in the response, and so cannot explain the persistence of the spectral shift Δ.

We conjecture that the response which forms the image should be regarded as a many-body process in the form of a surface-plasmon displacement. Other researchers have also modeled the coupling in terms of surface plasmons.[30] The effect on the photoelectron spectrum is to create plasmon sidebands at integral displacements of the surface-plasmon energy $\hbar\omega_p$. A theory of this process is closely analogous to that (see Ref. 25) for phonon creation in optical excitations. One finds a surface-plasmon sideband spectrum

$$I(E)=\sum_p \frac{S^p}{p!}e^{-S}\delta(E-p-\hbar\omega_p)\ ,$$

in which $S=\Delta/\hbar\omega_p$. No significant temperature dependence is expected, since $\hbar\omega_p \gg kT$. In experiments with transition metals, where $\hbar\omega_p \sim 10$ eV, the plasmon satellites would be weak and far removed from the main line (here set at $E=0$). For Ar on Cs one has $S\simeq 1$, so that the structure may be readily observable.

C. Optical line shapes

The optical line shapes reported in Sec. III warrant further brief comment. Phenomena of particular interest are the threshold profile and the pair peaks. Neither of these effects can be explained in any detailed way at present.

In some of the spectra the absorption immediately above threshold appears to increase quite linearly with photon energy, while in other cases small upward or downward curvatures are visible on a basically linear increase. This continuum absorption certainly has its origin in the conduction-electron response. Similar linear threshold profiles have been reported for rare-gas atoms in the bulk of metals,[20] and also in the response of alkali atoms in certain simple metallic environments.[32] The absence of the threshold singularities predicted, e.g., by MND theory,[15] remains unexplained, but the consistency between the present surface adsorbate results and earlier bulk alloy observations confirms the challenge these effects present to existing theories of the conduction-electron response.

No explanation from first-principles theory has been given for the rare-gas pair peaks. It appears certain that these sharp peaks occur when two rare-gas atoms occupy neighboring sites which are coupled to a conduction-electron liquid. The lack of broadening exhibited by the lines indicates that the transitions cause little or no shake-off excitation in the conduction-electron system. This may account in part for the prominence of the lines since they apparently offer a channel free from conduction-electron overlap effects. It warrants emphasis that the surface processes are remarkably similar to those reported a number of years ago for bulk alkali–rare-gas alloys.[20] For example, the spectrum of 4.6×10^{14} cm^{-2} Xe on Cs in Fig. 4 has exactly the same principal features as that for 29% Xe alloyed into Cs, including the pair-peak amplitude and width.[20] Similar phenomena have been discussed by Demuth *et al.*[12] on the basis of electron-energy-loss spectra.

ACKNOWLEDGMENTS

The authors thank T.-H. Chiu for his valuable assistance in certain experiments. Helpful discussion with E. Burstein, T. C. Chiang, J. E. Demuth, W. Eberhart, N. D. Lang, and A. Zangwill are acknowledged. This research was supported by the National Science Foundation Grant No. DMR-80-08139; use of facilities supported by the University of Illinois Materials Research Laboratory under Grant No. DMR-80-20250 is also acknowledged. This work was performed at the University of Wisconsin Synchrotron Radiation Center; thanks are due to the staff of the Synchrotron Radiation Center for their assistance. Parts of the interpretation and writing took place while one of us (D.G.) was supported by Contract No. DE-AC02-76CH00016, with the Division of Materials Sciences of the U.S. Department of Energy at Brookhaven National Laboratory.

APPENDIX: MANY-ELECTRON RELAXATION EFFECTS IN RARE-GAS SPECTRA

It has been emphasized throughout this paper that serious errors of interpretation can occur if a careful account is not taken of many-particle relaxation energies (e.g., the image energy) when discussing the one-electron orbital energies of adsorbed systems. An unfortunate example concerns Ar on Al, for which both photoemission[14] and optical excitation[10,21] from the $3p$ shell have been reported. As demonstrated in Sec. II, the main information contained in the photoemission and optical threshold energies, other than well-known atomic properties, is the image energy in photoemission [see Eq. (3)], and, in optical absorption, the excited-state bonding to the metal [see Eq. (1)]. The observed thresholds have nevertheless been employed erroneously as the basis for comparisons of single-particle properties of metal-adsorbate complexes.[14]

In the particular example of Ar on Al, the measured work function was 4.3 eV and the photoelectron threshold occurred at 9.8 eV below E_F. In other work,[10,21] the $3p_{3/2}\rightarrow 4s$ transition was observed to peak near 11.6 eV. Figure 10(a) was constructed by Lang *et al.*[14] to show that the Ar $3p_{3/2}$ level lies at -14.1 eV and that the Ar $4s$ level lies above the Al Fermi level. The correct way to draw the figure is given in Fig. 10(b), which leads to an entirely contrary conclusion.

One of the main problems with the analysis leading to Fig. 10(a) is that the *excited-state* bonding (image energy) is erroneously included in the determination of the $3p$ orbital energy of the *ground* configuration. When $\Delta=1.9$ eV is included in Fig. 10(b), as in Fig. 1, the Ar $3p_{3/2}$ orbital is located instead at $-14.1-1.9=-16.0$ eV. This improved interpretation is in good agreement with the known value -15.8 eV of the $3p_{3/2}$ binding for the *atom,* and with the fact that the Ar atom and Al metal hardly interact at all in the ground configuration, so that large core-energy shifts are not reasonable.

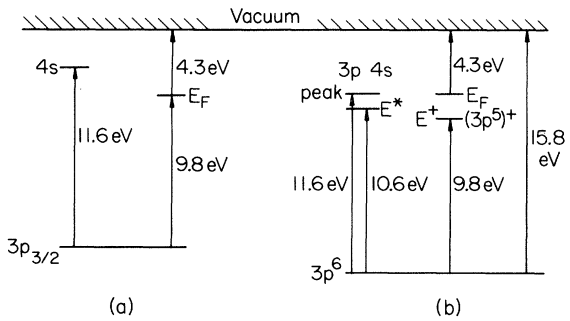

FIG. 10. Total energy of Ar on Al in various configurations. (a), as constructed by Lang *et al.* (Ref. 14) adds the $3p$ Ar photoelectron threshold at 9.8 eV below E_F to the 4.3-eV work function to find the $3p$ level at -14.1 eV. Then the 11.6-eV optical $3p \rightarrow 4s$ peak is interpreted to indicate that the $4s$ line "lies above E_F." The corrected diagram (Ref. 13) is shown in (b). It relates to the charge transfer energy $E^+ - E^*$, rather than to a comparison of E_{4s} with E_F. From other considerations E_{4s} can be shown to lie well *below* E_F.

A second difficulty is that the one-electron energy of the $4s$ orbital has been calculated with two errors. The broadly peaked optical profile can only be due to excitations of the conduction electrons (and perhaps phonons). Rather than the *peak* near 11.6 eV, it is the excitation *threshold* near 10.6 eV which locates the $4s$ level with the system otherwise unexcited. In addition, this energy must be measured relative to the 16.0-eV $3p_{3/2}$ level, rather than relative to the incorrect value of 14.1 eV. Our improved calculation thus correctly places the $4s$ level near $E_{4s}=16.0-10.6=5.4$ eV below the vacuum level. This is in good agreement with the atomic binding energy of the $4s$ orbital, namely $I^*=4.21$ eV, when augmented by K-like bonding, with $\epsilon_K=0.93$ eV of Ar* to the Al surface. The estimate is therefore $E_{4s}=4.21+0.93=5.14$ eV below vacuum. The agreement with the deduced 5.4-eV value would be almost exact if the atomic $3p_{3/2}$ level at -15.76 eV were taken instead of the value -16.0 eV deduced from the photoemission result. Note that throughout we neglect core polarization, and ascribe the entire valence energy for one-electron atoms to the single valence electron.

A final confusion brought about by Fig. 10(a) is that the Fermi energy is not correctly placed because the many-particle work function $\phi=4.3$ eV is used in place of the single-particle energy. What a comparison of $E_{4s}=5.1$ eV with $\phi=4.3$ eV actually signifies is that $5.1-4.3=0.8$ eV would be needed to transfer an electron from the $4s$ level to E_F, *provided that the conduction electrons were held frozen.* An actual transfer would involve the ion and screening, and thus entail the gain of an image energy of about 1.9 eV, so that the ionic configuration actually lies below the neutral configuration in total energy by $1.9-0.8=1.1$ eV. This is roughly the result indicated in Table II for Ar on Al. The question of the single-particle conduction-state energies at E_F and whether or not they mix with the $4s$ Ar adsorbate level is more difficult to assess. It will be discussed in paper II.[21]

Other researchers have thought,[14] in addition, that direct calculations of the $4s$ orbital energy, using density-functional methods confirm the assignment of an energy above E_F to the excited orbital of the Ar adsorbate. The density functional method is known to work very well for the ground state. In the case of Ar on Al, the electron and hole localize together on one site. In the reported calculations, however, the excited electron is scattered off the ground state, together with the core hole *and its image potential;* the spurious image effect then throws the scattering resonance much too high in energy, and leads to deductions about its relationship to E_F which are not reliable. These calculations place the orbital about 2.5 eV below the energy zero,[14] whereas it actually lies about 5.1 eV below zero, as demonstrated above. The error of $5.1-2.5=2.6$ eV is not too different from the interaction of the Ar electron with the image potential $2\Delta \simeq 3.8$ eV, which the method of calculation introduces erroneously into the vicinity of the Ar cell.

*Permanent address: Physics Department, Brookhaven National Laboratory, Upton, New York 11973.

[1]See, e.g., B. E. Nieuwenhus, O. G. Van Aardenne, and W. H. M. Sachtler, Chem. Phys. 5, 418 (1974); C. Mavroyannis, Mol. Phys. 6, 593 (1963).

[2]G. Ehrlich and F. G. Hudda, J. Chem. Phys. 30, 493 (1959).

[3]See, for example, T. Gustafsson, and E. W. Plummer, in *Photoemission and the Electronic Properties of Solids,* edited by B. Feuerbach, B. Fitton, and R. F. Willis (Wiley, New York, 1978), pp. 353–379, and references therein. Also, J. F. Herbst, Phys. Rev. Lett. 49, 1586 (1983).

[4]T. C. Chiang, G. Kaindl, and D. E. Eastman, Solid State Commun. 41, 661 (1982).

[5]G. Kaindl, T. C. Chiang, D. E. Eastman, and F. J. Himpsel, Phys. Rev. Lett. 45, 1808 (1980).

[6]B. J. Waclawski and J. F. Herbst, Phys. Rev. Lett. 35, 1594 (1975); J. F. Herbst, Phys. Rev. B 15, 3720 (1977).

[7]K. Horn, M. Scheffler, and A. M. Bradshaw, Phys. Rev. Lett. 41, 882 (1978).

[8]J. W. Gadzuk, S. Holloway, C. Manani, and K. Horn, Phys. Rev. Lett. 48, 1288 (1982).

[9]N. D. Lang, Phys. Rev. Lett. 46, 842 (1981).

[10]J. E. Cunningham, D. K. Greenlaw, and C. P. Flynn, Phys. Rev. Lett. 42, 328 (1979); Phys. Rev. B 22, 717 (1980).

[11]W. Eberhardt and A. Zangwill, Phys. Rev. B 28, 5960 (1983).

[12]J. E. Demuth, Ph. Avouris, and D. Schmeisser, Phys. Rev. Lett. 50, 600 (1983).

[13]C. P. Flynn and J. E. Cunningham, J. Phys. C 15, L1169 (1982).

[14]N. D. Lang, A. R. Williams, F. J. Himpsel, B. Reichl, and D. E. Eastman, Phys. Rev. B 26, 1728 (1982).

[15]G. D. Mahan, in *Solid State Physics,* edited by F. Seitz, D. Turnbull, and H. Ehrenreich (Academic, New York, 1974), Vol. 29.

[16]G. D. Mahan, Phys. Rev. 163, 612 (1967); P. Nozieres and C. T. de Dominicis, *ibid.* 178, 1097 (1969). For a comprehensive review see Ref. 15.

[17]S. Donaich and M. Sunjic, J. Phys. C 3, 285 (1970).

[18]J. W. Wilkins, in *X-ray and Atomic Inner-Shell Physics—1982 (International Conference, University of Oregon),* proceedings of the International Conference on X-Ray and Atomic Inner-Shell Physics, edited by B. Crasemann (AIP, New York, 1982), p. 687.

[19]P. H. Citrin, G. K. Wertheim, and M. Schluter, Phys. Rev. B 20, 3067 (1979).

[20]D. J. Phelps, R. A. Tilton, and C. P. Flynn, Phys. Rev. B 14, 5254 (1976); 14, 5265 (1976); 14, 5279 (1976).

[21]J. E. Cunningham, Doon Gibbs, and C. P. Flynn, following paper, Phys. Rev. B 29, 5304 (1984).

[22]J. C. P. Mignolet, J. Chem. Phys. 21, 1298 (1953); H. H. Rotermund and K. Jacobi, Surf. Sci. 126, 32 (1983). Recent unpublished measurements of the work-function change induced by Xe on Cs by Y. C. Chen indicate small changes at submonolayer coverages, in contrast to the essentially zero result reported in Ref. 1.

[23]See, e.g., C. P. Flynn, J. Phys. F 10, L315 (1980).

[24]J. Holz and F. K. Schulte, *Solid State Physics: Work Function of Metals,* Vol. 85 of *Springer Tracts in Modern Physics* (Springer, New York, 1977), pp. 1—150.

[25]T. Yakohawa and O. Kleppa, J. Phys. Chem. Solids 40, 46 (1964).

[26]For a general treatment, see A. M. Stoneham, *Theory of Defects in Solids* (Oxford University Press, New York, 1975). Core excitations in metals are discussed by C. P. Flynn, Phys. Rev. Lett. 37, 1445 (1976); B. Johannson and N. Martensson, Phys. Rev. B 21, 4427 (1980).

[27]F. Seitz, *Modern Theory of Solids* (McGraw-Hill, New York, 1940).

[28]Valuable discussions are given by I. Lindau, *X-Ray and Atomic Inner-Shell Physics—1982 (International Conference, University of Oregon),* proceedings of the International Conference on X-Ray and Atomic Inner-shell Physics, Ref. 18, p. 559; C. Noguera, *ibid.,* p. 676.

[29]K. Shinjo, S. Sugano, and T. Sasada, Phys. Rev. B 28, 5570 (1983), employ the adsorbate model of K. Schonhammer and O. Gunnarson, Solid State Commun. 26, 399 (1980).

[30]J. D. E. McIntyre and D. E. Aspnes, Surf. Sci. 24, 417 (1971).

[31]C. E. Moore, *Atomic Energy Levels,* Natl. Bur. Stand. (U.S.) Circ. No. 35 (U.S. GPO, Washington, D.C. 1971).